ChemEngineering

MDPI

*Article*

# Catalyst Effects on the Pyrolysis Kinetics of Major Textile Wastes: Cotton, Polyester, and Nylon

**Peyman Alizadeh [1], Mahtab Sultany [1], Sarah Chen [1], Taylor Wright [2], Preksha Sharma [2] and Xiaotao Bi [1,*]**

[1] Chemical and Biological Engineering Department, University of British Columbia, Vancouver, BC V6T 1Z3, Canada
[2] Lululemon Athletica, 1818 Cornwall Avenue, Vancouver, BC V6J 1C7, Canada
* Correspondence: tony.bi@ubc.ca

**Abstract**

This study examines how catalysts and operating conditions enhance the pyrolysis of textile wastes, supporting their use as a viable feedstock for waste-to-energy recycling. Pyrolysis of three common textile wastes—cotton, polyester, and nylon—was studied using thermogravimetric analysis (TGA). Experiments were conducted at heating rates of 5, 10, 15, and 20 °C/min, both with and without catalysts, including $K_2CO_3$, ZnO, KOH, CaO, and natural zeolite. The results showed that cotton decomposes at significantly lower temperatures than polyester and nylon, with a peak decomposition rate at 361.7 °C compared to 437.9 °C for polyester and 459.8 °C for nylon. Reaction kinetics were analyzed using three established models: Kissinger–Akahira–Sunose (KAS), Flynn–Wall–Ozawa (FWO), and Kissinger. Among the materials studied, polyester exhibited the lowest activation energy (184.8 kJ/mol), while cotton and nylon showed higher values (241.1 and 236.2 kJ/mol, respectively). Catalyst performance varied by material. Potassium carbonate was particularly effective for cotton, increasing the weight loss rate and reaction rate constant. ZnO significantly reduced the activation energy for nylon. Although catalysts generally enhanced reaction rates, many also increased activation energy. This increase in activation energy and collision frequency suggests that catalytic pyrolysis becomes more temperature-sensitive while achieving higher reaction turnover frequencies.

**Keywords:** pyrolysis; textile waste; catalysts; kinetics; thermochemical decomposition



Academic Editor: Dmitry Yu. Murzin

Received: 28 February 2026
Revised: 15 April 2026
Accepted: 6 May 2026
Published: 13 May 2026



## 1. Introduction

Post-consumer textile waste has become a serious issue: despite the fact that more than 95% of post-consumer material could be recycled, only 15% is recycled and two-thirds of it ends up in landfill [1]. The primary concerns of landfilling textile waste are pollution of soil and groundwater by heavy metals present in the dye components in the manufactured textiles [2]. Every year, an estimated 190,000 tons of microfibers from synthetic fabrics, largely comprised of petroleum-based polymers, are estimated to be deposited in the ocean [3]. Synthetic microfibers, a major source of pollution, are projected to account for up to 35% of microplastics in water bodies, with a large portion contributed by fabric microfibers [4]. There is an enormous amount of cotton in textile waste, but since the cotton is mixed with other materials (such as dyes and polymer fibers), it is difficult to recover it economically [5]. The same issue is occurring for polyester and nylon.

In many densely populated cities, converting textile waste into energy could partially fulfill energy needs, which is especially beneficial since textile waste as an energy source

could be 70–80% cheaper than oil, wood pellets and wood chips [6]. There are several methods to convert waste to energy: thermochemical, biochemical, and physicochemical. Pyrolysis (as one of the thermochemical methods) is one promising way to convert waste synthetic polymers and biomass wastes into gaseous fuel, liquid fuel, and charcoal via slow or fast pyrolytic approaches [7]. Unlike mechanical and chemical processing, pyrolysis is capable of treating nearly all kinds of synthetic polymers and their mixes.

The thermochemical conversion of textile waste has recently drawn attention as a potentially effective method to recycle textile waste to bioenergy and biofuels [8–10]. Using a thermogravimetric analyzer (TGA), Molto et al. [11] examined the thermal decomposition of cotton fabric samples in an inert atmosphere and suggested a two-step kinetic model to explain the thermal cracking of cotton waste. Zhu et al. [12] studied the thermal conversion of ramie fabric waste for energy in a TGA unit at heating rates of 5, 10, 20 and 40 °C $min^{-1}$. The reaction kinetics was examined by comparisons between isoconversional model-free methods (e.g., Coats–Redfern method) and one model-fitting method. Wen et al. [13] used a Thermogravimetric–Fourier-Transform-Infrared-Spectroscopy (TG-FTIR) system to study the pyrolysis kinetics of three types of textile waste and their mixture—polyester, wool and cotton—under a $CO_2$ environment at a temperature range of 300–500 °C.

To improve the pyrolysis reaction rate and the pyrolysis oil quality, catalysts such as $Al_2O_3$, CuO, ZnO and $Fe_2O_3$ can be applied. For example, Wu et al. [14] reported a 35% decrease in the pyrolysis reaction activation energy with the use of a ZnO catalyst. Pyrolysis using catalysts can also boost liquid yields from textiles (blue and black jeans) [5]. The catalytic pyrolysis of textiles (cotton and polyester) was carried out at pilot scale, utilizing $Al_2O_3$ at 800 °C. The typical yields of char, gas and oil were 17.8, 44.0 and 37.5%, respectively [5]. The pyrolysis of polyethylene terephthalate (PET) was investigated at temperatures of 400–550 °C [15]. Due to its low thermal conductivity and low melting temperature, it was recommended that a proper reactor design (e.g., fluidized bed) and catalyst (e.g., ZnO) be applied to increase heat transfer and minimize agglomeration.

The selection of catalysts in this study was based on their distinct and well-documented chemical functionalities in thermochemical conversion processes. Alkali-based compounds such as $K_2CO_3$ and KOH possess strong basicity and are known to promote dehydration, depolymerization, and char–gas reactions in lignocellulosic and polymeric materials, thereby facilitating bond cleavage and accelerating thermal decomposition. CaO, a basic oxide, has been widely reported to enhance secondary cracking reactions, capture acidic gases, and improve tar reforming behavior during pyrolysis. ZnO, a metal oxide with Lewis acidic character, has demonstrated strong catalytic activity for chain scission and depolymerization of polyester- and PET-like polymers, while natural zeolite provides acidic and porous active sites that promote cracking and vapor upgrading. These low-cost and industrially accessible catalysts were therefore selected to represent a range of catalytic functionalities (alkaline, basic oxide, metal oxide, and acidic porous catalysts) and to systematically evaluate their interactions with three major textile fibers (cotton, polyester, and nylon).

Although catalytic pyrolysis of textile waste has been widely investigated, most previous studies have focused on single textile types, specific catalysts, or product characterization [16]. A systematic comparison of the kinetic behavior of the three dominant textile fibers—cotton, polyester, and nylon—under identical experimental conditions using multiple low-cost catalysts remains limited. The novelty of this study lies in (i) the direct comparison of catalytic effects across natural and synthetic textile fibers, (ii) the evaluation of inexpensive and industrially accessible catalysts representing different catalytic functionalities, and (iii) the identification of catalyst-dependent kinetic compensation effects, where activation energy and pre-exponential factor vary simultaneously. This comparative

kinetic framework provides insight into catalyst–fiber interactions that cannot be obtained from single-material studies.

These three fabrics have been chosen as they are the most common feedstock for the apparel industry and the post-consumer waste resulting from their processing is substantial. Our ultimate goal is to develop a microwave-assisted fluidized bed pyrolysis reactor for the catalytic pyrolysis of a waste textile mix. Based on our previous study on microwave-assisted catalytic pyrolysis of biomass residues, we selected $K_2CO_3$ for catalytic pyrolysis of cotton at two different ratios of 10 and 20%; ZnO, CaO, KOH, and natural zeolite for polyester; and ZnO, which has been reported to be effective in catalyzing the cracking of low-melting temperature plastics, e.g., PET, to prevent agglomeration, for nylon. The objective of this study is to identify suitable pyrolysis temperature ranges and effective catalysts to decompose these three major textile wastes, with their reaction kinetics established for assisting the design and simulation of pyrolysis reactors, and to discover the best textile for pyrolysis compared to others. Also, the established reaction kinetics for selected catalysts on each textile will provide us a reference for our future study on blended waste textile mixtures.

## 2. Materials and Methods

### *2.1. Feedstock and Catalysts*

Cotton, nylon 6 and polyester samples (100% pure) were provided by Lululemon (Vancouver, BC, Canada) in various colors, but only undyed (white) and dyed (black) samples were tested. The samples of cotton, nylon and polyester (150 $g/m^2$) were shredded using a shredding machine. Clinoptilolite (or natural zeolite) from KMI-zeolite and $K_2CO_3$, ZnO, KOH, and CaO from Sigma Aldrich were used as catalysts in the experiments. Catalysts were physically mixed with shredded textile samples at the specified mass ratios (10–20 wt% relative to textile mass). Mixing was performed manually using a mortar and pestle for approximately 10 min to ensure uniform distribution of catalyst particles within the textile matrix prior to TGA testing.

### *2.2. Thermogravimetry Analysis (TGA)*

The TGA experiments were conducted in a Shimadzu TGA-50 thermogravimetric analyzer (Mandel Scientific, Guelph, ON, Canada), located at the Department of Chemical and Biological Engineering at the University of British Columbia using shredded textile samples. All experiments were performed under an inert atmosphere using high-purity nitrogen (99.999%) at a flow rate of 50 mL/min to prevent oxidative reactions during thermal decomposition. Approximately 100 ± 0.5 mg of sample was placed in a quartz crucible for each experiment. The catalyst-to-sample ratio was maintained at a range [e.g., 1:5] to ensure sufficient microwave absorption for sample heating and to ensure sufficient active sites for the vapor-phase intermediate reactions without causing excessive thermal lagging, while the flow rate was optimized to minimize secondary reactions and ensure the immediate removal of volatiles, consistent with established protocols in biomass and plastic pyrolysis.

The samples were heated from room temperature to 700 °C at linear heating rates of 5, 10, 15, and 20 °C/min, followed by an isothermal holding period of 10 min to ensure completion of thermal decomposition. Sample mass was recorded at a frequency of 1 Hz throughout the experiment. The balance resolution of the instrument was 0.01 mg.

To ensure reproducibility of the measurements, selected experiments were conducted in duplicate. The variation in peak decomposition temperature (±3–5 °C) and total mass loss (±5%) between repeated runs was within typical experimental uncertainty for non-

isothermal TGA measurements. The reported thermal and kinetic parameters were obtained from consistent datasets across the investigated heating rates.

It should be noted that thermogravimetric analysis represents small-scale thermal decomposition under controlled heating conditions and does not replicate full reactor-scale pyrolysis behavior. In this study, TGA is employed as a kinetic screening tool to determine decomposition temperature ranges and apparent kinetic parameters, which serve as fundamental inputs for subsequent reactor design and simulation.

### 2.3. Methods

The solid-state thermal decomposition rate is determined by the temperature and reactant concentration. In the non-isothermal tests, the reaction continues at a specified heating rate β (K/min), while the sample weight is constantly tracked as a function of time. The fractional conversion is calculated by:

$$\alpha = \frac{w_0 - w_t}{w_0 - w_f} \quad (1)$$

where $w_t$, $w_o$, and $w_f$ represent the sample mass presented at a given time and the initial and final times, respectively. The non-isothermal decomposition reaction rate, denoted as $d\alpha/dt$, is determined by the rate at which conversion changes over time. At a linear temperature heating rate, two independent functions, namely conversion function ($f(\alpha)$) and temperature function ($k(T)$), describe the reaction kinetics, as given in Equation (2):

$$\frac{d\alpha}{dt} = \beta\frac{d\alpha}{dT} = k(T)f(\alpha) \quad (2)$$

The Arrhenius equation describes the dependency of the rate constant, k, on temperature:

$$k(T) = Aexp(-\frac{E_\alpha}{RT}) \quad (3)$$

The activation energy ($E_\alpha$) reflects the minimal energy required to initiate the reaction. A lower activation energy value indicates a greater probability of reactivity at lower temperatures.

The Kissinger method is a differential method, which relates the temperature values $T_m$ at the maximum reaction rate to the heating rate and activation energy by [17]:

$$\text{Ln } \beta/T^2_m = \text{Ln } \frac{AR}{E_\alpha} - \frac{E_\alpha}{RT_m} \quad (4)$$

The activation energy can be determined by the slope of $-E_\alpha/R$ (R = 8.31 J/mol·K) from a straight line of ln ($\beta/T_m$) versus 1/T.

The Kissinger–Akahira–Sunose (KAS) method in its simplified form is given by [17,18]. The method is an integral isoconversional technique that offers higher accuracy than the Kissinger method by not assuming a constant activation energy throughout the process. It is expressed as:

$$\text{Ln } \beta/T^2 = \text{Ln } \frac{AR}{E_\alpha} - \frac{E_\alpha}{RT} \quad (5)$$

The activation energy can be calculated from a plot of Ln $\beta/T^2$ versus 1/T for an assumed constant value of A, where the slope is equal to $-E_\alpha/R$.

The Flynn–Wall–Ozawa (FWO) method is an isoconversional, integral method and is given by the following standardized equation [19,20]:

$$\text{Ln } \beta = \text{Ln } \frac{AE_\alpha}{RF(\alpha)} - 5.331 - 1.052\frac{E_\alpha}{RT} \quad (6)$$

For a constant conversion, α, and pre-exponential factor, A, the plot of ln β vs. 1/T at several heating rates should give a straight line with a slope of −1.0527 $E_\alpha$/R. The activation energy can be estimated via the slope at a wide range of conversion, α.

The Coats–Redfern method belongs to a model-fitting method that involves the thermal degradation mechanism [21]. The simplified equation can be expressed as:

$$\text{Ln } F(\alpha)/T^2 = \text{Ln } \frac{AR}{\beta E_\alpha} - \frac{E_\alpha}{RT} \quad (7)$$

The activation energy can be estimated from the slope of the plot of ln($F(\alpha)/T^2$) vs. 1/T using a specific algebraic expression of F(α) for a given kinetic mechanism (Table 1). The pre-exponential factor A can then be calculated from the intercept ln ($AR/\beta E_\alpha$).

**Table 1.** Algebraic expressions, F(α), for the frequently used reaction mechanisms [22].

| Mechanism | Differential Form f(α) | Integral Form F(α) |
|---|---|---|
| Contracting sphere (R2) | $2(1-\alpha)^{1/2}$ | $1-(1-\alpha)^{1/2}$ |
| Contracting cylinder (R3) | $3(1-\alpha)^{2/3}$ | $1-(1-\alpha)^{1/3}$ |
| One-dimensional diffusion (D1) | $1/2\alpha$ | $\alpha^2$ |
| Two-dimensional diffusion (D2) | $[-\ln(1-\alpha)]^{-1}$ | $(1-\alpha)\ln(1-\alpha)+\alpha$ |
| Three-dimensional diffusion (D3) | $3(1-\alpha)^{2/3}/2[1-(1-\alpha)^{1/3}]$ | $[1-(1-\alpha)^{1/3}]^2$ |
| Ginstling–Brounshetein (D4) | $3/2[(1-\alpha)^{-1/3}-1]^{-1}$ | $1-(2\alpha/3)-(1-\alpha)^{2/3}$ |
| Power law (P2) | $2\,\alpha^{1/2}$ | $\alpha^{1/2}$ |
| Power law (P3) | $3\,\alpha^{2/3}$ | $\alpha^{1/3}$ |
| Power law (P4) | $4\,\alpha^{3/4}$ | $\alpha^{1/4}$ |
| Avarami-Erofe'ev (A2) | $2(1-\alpha)[-\ln(1-\alpha)]^{1/2}$ | $[-\ln(1-\alpha)]^{1/2}$ |
| Avarami-Erofe'ev (A3) | $3(1-\alpha)[-\ln(1-\alpha)]^{2/3}$ | $[-\ln(1-\alpha)]^{1/3}$ |
| Avarami-Erofe'ev (A4) | $4(1-\alpha)[-\ln(1-\alpha)]^{3/4}$ | $[-\ln(1-\alpha)]^{1/4}$ |

## 3. Results and Discussion

### 3.1. Pyrolysis of Single Species (Cotton, Polyester, and Nylon)

The proximate and ultimate analyses of polyester, cotton and nylon are shown in Table 2. Overall, the three samples were quite similar in elemental composition, with high carbon content and relatively low hydrogen content. The oxygen content is highest for cotton and lowest for nylon. The HHV of fabric samples using a bomb calorimeter ranges from 16.8 to 31 MJ/kg, with nylon as the highest, corresponding to it having the lowest oxygen content. Petroleum-based fibers like polyester, acrylic, and nylon have higher carbon content and HHV compared to other natural fabrics [23].

**Table 2.** Proximate and ultimate analyses of textile samples.

| Sample | Fixed Carbon (%) | Volatiles (%) | Ash Content (%) | HHV (MJ/kg) | C | H | N | S | O |
|---|---|---|---|---|---|---|---|---|---|
| Polyester (white) | 14.20 | 85.80 | 0 | 22.96 | 62.54 | 4.38 | 0 | 0 | 33.08 |
| (black) | 17.09 | 82.01 | 0.9 | 20.56 | 60.85 | 4.21 | 0 | 0 | 34.94 |
| Cotton (white) | 15.02 | 84.98 | 0 | 16.9 | 42.78 | 6.1 | 0 | 0 | 51.12 |
| (black) | 14.43 | 85.27 | 0.3 | 16.81 | 42.8 | 6.12 | 0 | 0 | 51.08 |
| Nylon (white) | 7.8 | 92.2 | 0 | 31.29 | 62.18 | 9.44 | 11.82 | 0 | 16.56 |
| (black) | 5.37 | 94.07 | 0.56 | 30.39 | 62.43 | 8.99 | 10.91 | 0 | 17.66 |

The weight loss (TG) and weight loss rate (DTG) graphs of different textiles (polyester, nylon and cotton) are shown in Figures 1 and 2. The heating rate was 10 °C/min. The

curves suggest that the pyrolysis of polyester occurs in only one stage; however, the cotton samples first lost a small amount of their weight (roughly 5–6%) below 100 °C and they lost most of their weight at the second stage. The first weight loss stage could be due to the evaporation of water and other volatile chemicals in cotton samples [5]. The second stage resulted from fiber decomposition. The decomposition of cotton samples occurred at lower temperatures (316–420 °C) compared to polyester (385–488 °C). Degradation of nylon samples took place at a similar temperature range as for polyester.

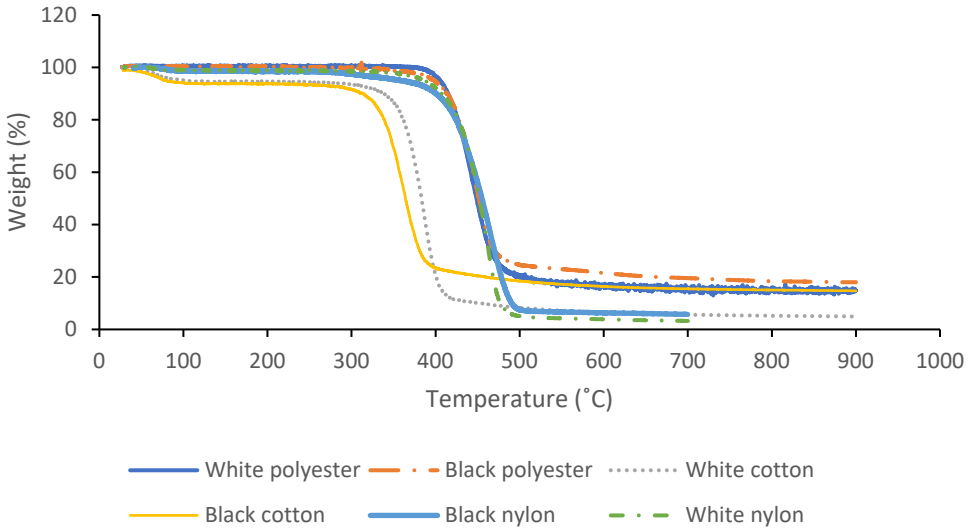


**Figure 1.** Pyrolysis TG curves of textile samples at a heating rate of 10 °C/min.

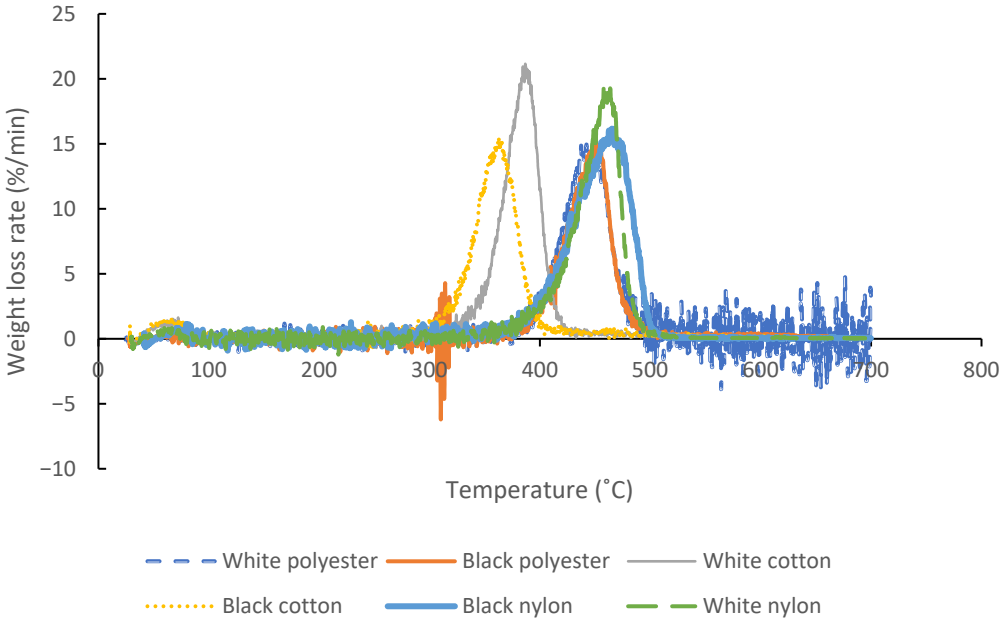


**Figure 2.** Pyrolysis DTG curves of textile samples at a heating rate of 10 °C/min.

It has been reported [24–27] that the thermal decomposition of PET started at temperatures of 360–400 °C, with the most prominent peak at ~428 °C. For example, Girija et al. [28] suggested that PET went through a single-stage decomposition with ~60% degraded at a temperature of 440 °C. The maximum amount of volatiles was released from the pyrolysis of black and white nylon (93.55 and 92.71%, respectively) (Table 3). Alhulaybi and Dubdub [29] showed that the pyrolysis of PET occurs at a temperature of 377 to 477 °C with about 20 wt% residue generation. The kinetic parameters presented in Table 3 were

determined at a heating rate of 5 °C/min. This specific rate was selected as the baseline for kinetic performance to align with the lowest heating rate utilized in the TGA experimental series, ensuring high resolution of the initial decomposition stages.

**Table 3.** Pyrolysis performance of polyester and cotton samples at a heating rate of 5 °C/min.

| Sample | Temperature at Maximum Weight Loss Rate (°C) | Maximum Weight Loss Rate (%/°C) | Weight Loss During Pyrolysis (%) |
|---|---|---|---|
| White polyester | 437.9 | 13.50 | 78.75 |
| Black polyester | 442.8 | 8.88 | 78.47 |
| White cotton | 361.7 | 15.21 | 90.38 |
| Black cotton | 359.8 | 8.36 | 86.75 |
| Black nylon | 465.4 | 9.37 | 93.55 |
| White nylon | 459.8 | 8.39 | 92.71 |

The activation energies of cotton, polyester and nylon pyrolysis extracted using both the Kissinger and FWO methods are presented in Tables 4 and 5. $E_\alpha$ ranges from 180 to 300 kJ/mol, and black polyester had the lowest activation energy (184.8 KJ/mol). Using the FWO method, the activation energy was found to fall in a similar range as obtained using the Kissinger method, with undyed cotton having the lowest value. Matsumura et al. [30] estimated the activation energy from the Arrhenius plot and it was 111.8 kJ/mol for PET, which was smaller than 142.6 kJ/mol for cotton. Yousef et al. [31] studied the pyrolysis behavior of buttons and their kinetic performance to convert them into energy and their original chemical components. The kinetic analysis revealed that the $E_\alpha$ of the pyrolyzed polyester was in the range of 152–202 kJ/mol, and for nylon it was 156–201 kJ/mol.

**Table 4.** Activation energies of different textile samples from the Kissinger method.

| Sample | $E_\alpha$ (kJ/mol) |
|---|---|
| White polyester | 202.7 |
| Black polyester | 184.8 |
| White cotton | 241.1 |
| Black cotton | 297.0 |
| White nylon | 218.9 |

**Table 5.** Activation energies at various fractional conversions (α) from the FWO method (unit: kJ/mol).

| Sample | α | | | | | | | | | Average |
|---|---|---|---|---|---|---|---|---|---|---|
| | 0.1 | 0.2 | 0.3 | 0.4 | 0.5 | 0.6 | 0.7 | 0.8 | 0.9 | |
| White cotton | 104.1 | 178.5 | 194.3 | 199.0 | 198.4 | 199.5 | 194.9 | 190.8 | 188.3 | 183.0 |
| White polyester | 233.2 | 237.2 | 236.5 | 235.1 | 233.8 | 238.8 | 237.5 | 240.1 | 243.5 | 237.3 |
| White nylon | 128.0 | 205.5 | 212.6 | 212.2 | 226.1 | 250.1 | 255.6 | 259.3 | 268.9 | 224.2 |

The activation energy values estimated by the KAS method, which is similar to the FWO method, at different fractional conversions for various textile samples are demonstrated in Figure 3. White polyester is seen to have very stable values at the full range of fractional conversions from 0.1 to 0.9 (average: 237 kJ/mol). Osman et al. [32] used the FWO method to show a variation in $E_\alpha$ during the pyrolysis of PET, which was in the range of 166–180 kJ/mol. Zhu et al. [12] calculated the activation energies of pyrolyzed ramie using the KAS and FWO methods (167 and 169 kJ/mol, respectively), which were lower than the $E_a$ of pyrolyzed textile waste using the same methods.

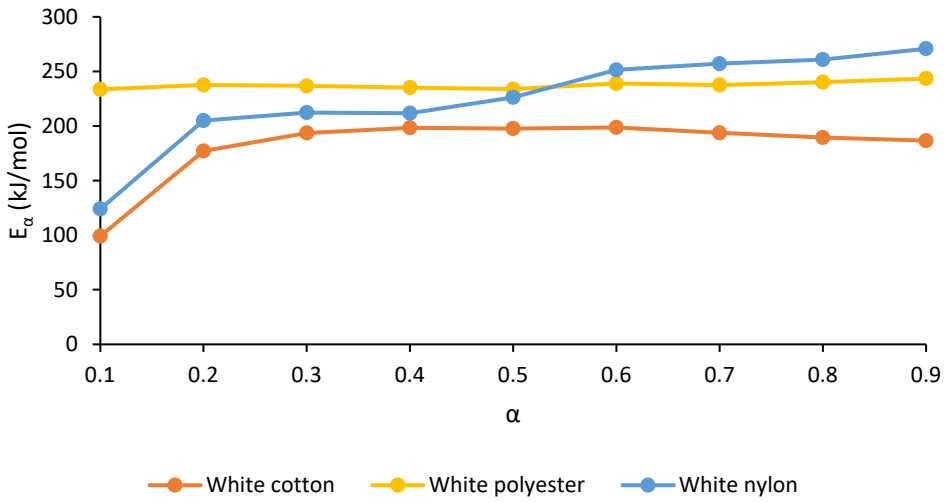


**Figure 3.** Activation energies of undyed cotton, polyester and nylon at different fractional conversions obtained via the KAS method.

To elucidate the reaction mechanism of pyrolysis of different textile waste, the activation energy was extracted by the Coats–Redfern method based on different pyrolysis reaction mechanisms, with the $E_\alpha$ values of undyed cotton, polyester and nylon at different heating rates displayed in Figures 4–6. It is believed that a likely mechanism will have an $E_\alpha$ value close to that obtained using other methods (e.g., Kissinger or FWO). It is seen that for white polyester and white cotton, the $E_\alpha$ values from the R2 and R3 mechanisms are closest to the values obtained from Kissinger and FWO methods, suggesting that polyester and cotton likely followed the reaction mechanism R3, a contracting cylinder, or R2, a contracting sphere. On the other hand, white nylon likely followed the mechanism model of D1 (one-dimensional diffusion). The difference is possibly related to the much lower oxygen content in nylon than in cotton and polyester. The mechanism for pyrolyzed ramie was a phase-boundary-controlled reaction type (R2 or R3) [12].

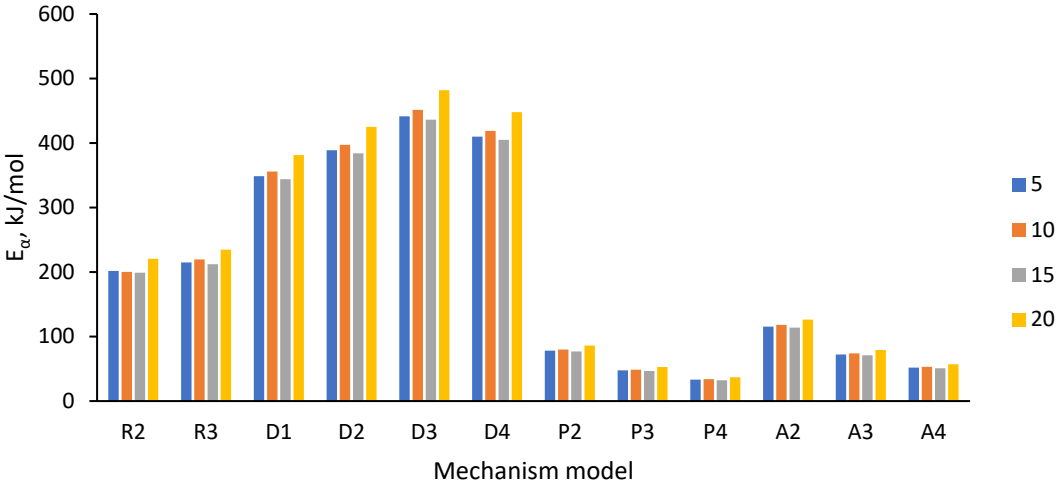


**Figure 4.** Relationship between estimated $E_\alpha$ and reaction mechanisms for pyrolysis of white polyester as estimated by the Coats–Redfern method.

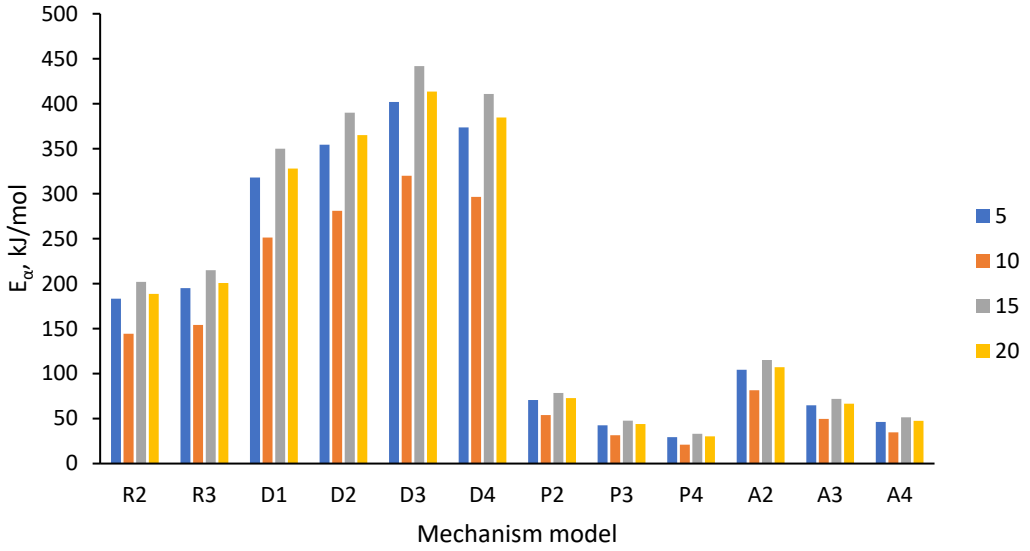


**Figure 5.** Relationship between estimated $E_\alpha$ and reaction mechanisms for pyrolysis of white cotton as estimated by the Coats–Redfern method.

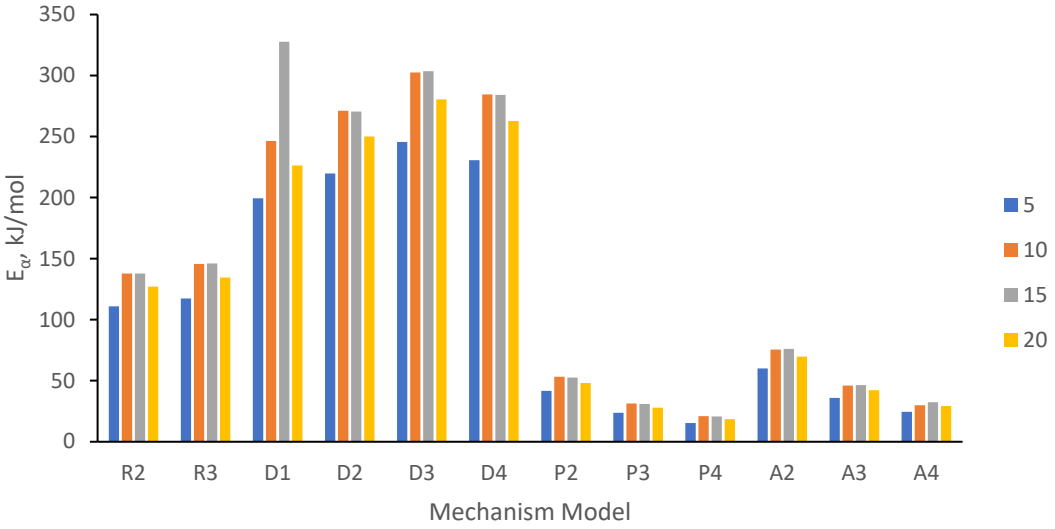


**Figure 6.** Relationship between estimated $E_\alpha$ and reaction mechanisms for pyrolysis of white nylon as estimated by the Coats–Redfern method.

### *3.2. Catalytic Pyrolysis of Single Species (Cotton, Polyester, and Nylon)*

Pure textile materials were intentionally used in this study to isolate the intrinsic thermal and catalytic behavior of individual fiber types. Real post-consumer textile wastes typically contain blends, dyes, and additives that introduce additional complexity and variability. While absolute kinetic values may differ for mixed wastes, the relative trends observed here provide a fundamental basis for understanding catalyst–fiber interactions in more complex waste streams.

For the pyrolysis of white polyester with 20% KOH, the starting temperature, temperature at maximum weight loss rate and ending temperature all increased with the increase in heating rate, and the pyrolysis temperature range became wider (Figure 7). However, as shown in Figure 8, the heating rate had little effect on the total mass loss (or yield of solid residue).

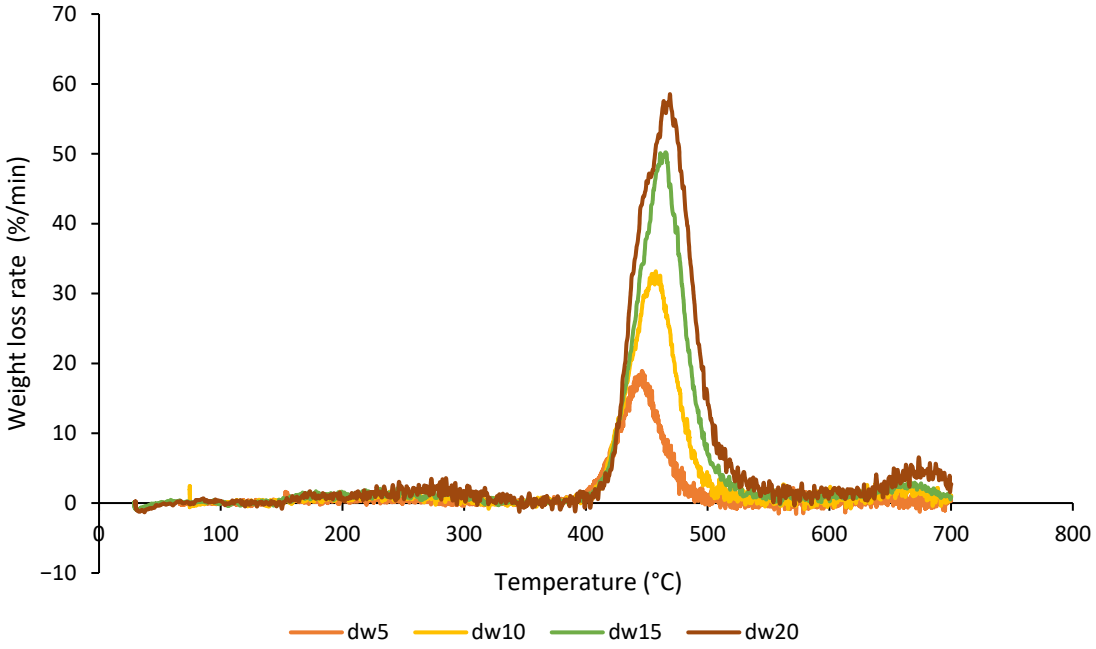


**Figure 7.** Pyrolysis DTG curves of white polyester with 20% KOH at different heating rates. The notion "dw" refers to the derivative of weight (DTG) at specific heating rates.

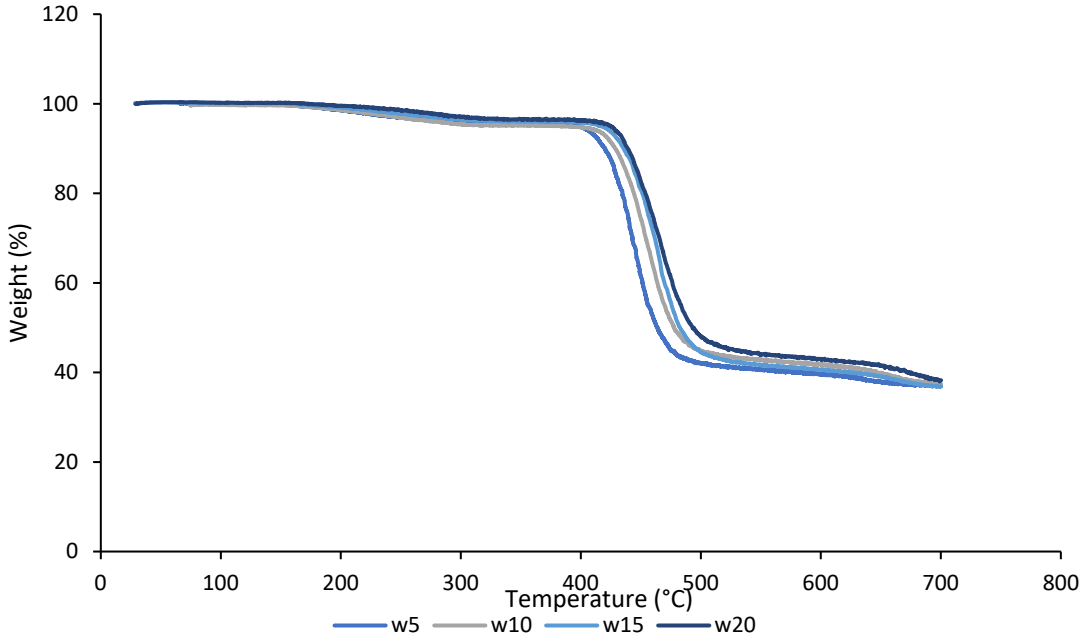


**Figure 8.** Pyrolysis TG curves of white polyester with 20% KOH at different heating rates.

The catalytic performance observed in the mixed textile systems (e.g., polyester–cotton blends) differs significantly from those of the single-component materials. In single-component pyrolysis, the catalyst interacts directly with a uniform decomposition pathway. However, in the mixed system, the presence of cellulose-derived volatiles from cotton may undergo cross-linking or synergistic reactions with the polyester-derived monomers on the catalyst surface. For instance, the alkaline sites of CaO show higher activity in deoxygenating the mixed vapors compared to the single-component runs, suggesting that the catalyst effectively manages the more complex intermediate products generated by the interaction of different polymer chains. This synergy is crucial for achieving consistent bio-oil quality in heterogeneous textile waste streams.

The influence of catalysts on TGA behavior can be interpreted through combined chemical and physical effects. Chemically, alkaline catalysts ($K_2CO_3$ and KOH) can promote dehydration, depolymerization, and fragmentation reactions, particularly for oxygen-rich cellulose-based fibers (cotton). Physically, the presence of solid catalyst particles can improve heat transfer within poorly conductive textile matrices, change melt viscosity and volatilization pathways (especially for polyester/nylon), and modify transport of evolved volatiles away from the sample surface. Therefore, a catalyst may shift the DTG peak temperature and change the apparent kinetic parameters ($E_\alpha$ and A) depending on which chemical pathway becomes dominant and whether mass/heat transport limitations are altered.

The pyrolysis characteristics of the three textile species are summarized in Table 6. White cotton with 20% $K_2CO_3$ was subjected to a maximum total weight loss (97%) at a heating rate of 5 °C/min. The highest solid residues were generated from the pyrolysis of white and black polyesters. Using catalysts increased the maximum weight loss rate for all tested textile species, which is more apparent for the pyrolysis of white cotton with 10% $K_2CO_3$. Also, the temperature at maximum weight loss rate increased for cotton and polyester with catalysts compared to the control (pure) and decreased for nylon. An increase in $T_m$ can occur when the catalyst promotes competing reaction pathways such as dehydration/condensation and char stabilization, or when stronger interactions between the catalyst and polymer fragments delay volatilization. For melting polymers, catalyst particles can also influence melt-phase transport and volatilization, producing either earlier or delayed peak decomposition depending on the balance between catalytic cracking and transport resistance.

**Table 6.** Pyrolysis performance of cotton, polyester and nylon at a heating rate of 5 °C/min.

| Sample | Temperature at Maximum Weight Loss Rate (°C) | Maximum Weight Loss Rate (%/°C) | Total Weight Loss During Pyrolysis (%) |
|---|---|---|---|
| White polyester | 437.9 | 13.50 | 78.75 |
| White polyester (KOH:20%) | 446.0 | 18.88 | 70.13 |
| White polyester (Zeolite:20%) | 449.9 | 47.28 | 78.33 |
| White polyester (ZnO:20%) | 439.0 | 19.56 | 83.38 |
| White polyester (CaO:20%) | 439.3 | 30.84 | 77.03 |
| White cotton | 361.7 | 15.21 | 90.38 |
| White cotton ($K_2CO_3$:10%) | 377.2 | 20.09 | 97.24 |
| White cotton ($K_2CO_3$:20%) | 376.0 | 18.73 | 88.31 |
| White nylon | 459.8 | 8.39 | 92.71 |
| White nylon (ZnO:20%) | 428.2 | 16.95 | 94.62 |

Catalyst weight is commonly subtracted to obtain the weight loss of the sample by assuming that the weight of the catalyst does not change during the pyrolysis. However, if the catalyst weight changes during pyrolysis, its weight loss should be accounted for in the data analysis. To evaluate the changes in weight of catalysts during pyrolysis, each catalyst alone was subjected to the heating process at the same heating rate with the same carrier gas, with their behavior demonstrated in Figure 9. Among the five types of catalysts, KOH had the highest weight loss during pyrolysis, which was around 30%, and ZnO and natural zeolite had a similar weight loss of 10 to 11%. $K_2CO_3$ was stable throughout the experiment, while the total weight loss of CaO was ~8%. To check the stability of the samples at temperatures with no expected catalyst decomposition, the catalyst samples were put into an oven and heated up to 250 °C. The resulting weight losses are shown in Table 7. It is seen that zeolite and ZnO had a weight loss of ~10%, likely from the removal

of water, while KOH gained weight (8%), likely due to the conversion of KOH to $K_2CO_3$ via reacting with $CO_2$ present in the atmospheric air.

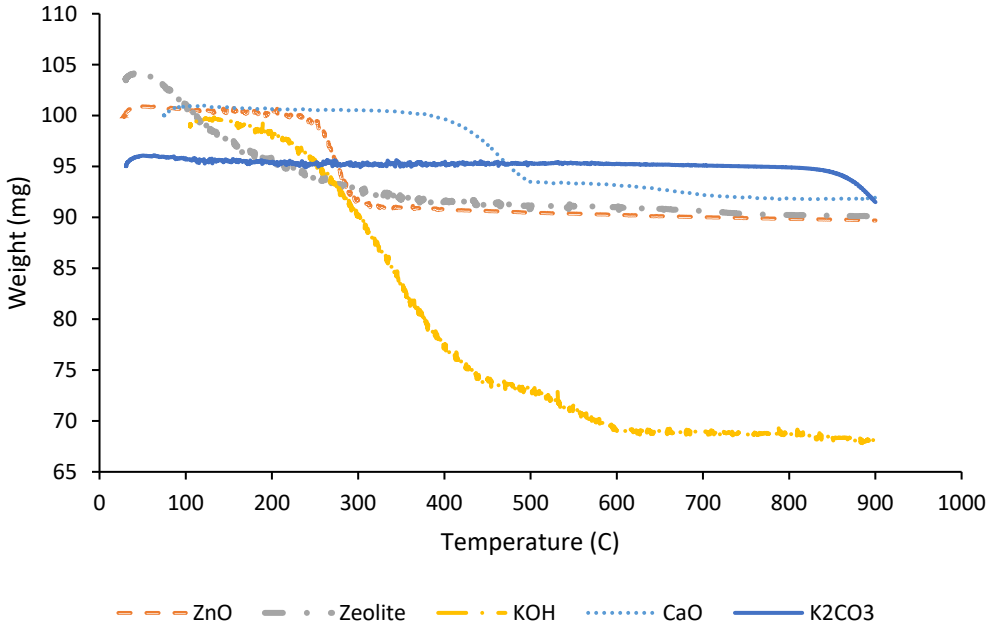


**Figure 9.** Weight loss of catalysts alone during pyrolysis.

**Table 7.** Weight change in catalysts after exposure to air in an oven at 250 °C for 24 h.

| Catalyst | Weight Change (%) |
|---|---|
| KOH | 8.25 |
| $K_2CO_3$ | 0.00 |
| Zeolite | −9.78 |
| ZnO | −11.30 |
| CaO | 0.9 |

As observed in Figure 9, the initial mass of the catalyst, particularly KOH, exhibited a slight increase at the beginning of the pyrolysis process. This is attributed to the hygroscopic nature of KOH, leading to the rapid absorption of atmospheric moisture ($H_2O$) and carbon dioxide ($CO_2$) during the sample loading and initial heating phases. The interaction with $CO_2$ results in the formation of potassium carbonate ($K_2CO_3$), which accounts for the recorded mass gain before the onset of the primary thermal decomposition of the polymer matrix.

To ensure the accuracy of the kinetic parameters, the TGA curves were corrected by subtracting the independent weight loss profile of the catalyst (measured under identical conditions) from the catalyst–sample mixture. This normalization isolates the degradation behavior of the textile components from the catalyst's own thermal changes (e.g., moisture loss or carbonation).

The activation energies of catalytic pyrolysis of undyed polyester, nylon and cotton were estimated using the Kissinger method, with the data summarized in Table 8. The lowest $E_\alpha$ was obtained from white nylon with ZnO (125.9 kJ/mol), and the highest $E_\alpha$ from white polyester with ZnO as the catalyst (345.5 kJ/mol). The results of Table 8 show that the addition of a catalyst could increase the activation energy, which is contrary to the data in the literature [14]. Yang et al. [33] studied the pyrolysis behavior of three types of biomass (sawdust, cellulose and straw) in the absence of a catalyst and in the presence of Ni-$Ca_2SiO_4$ and Ni-CaO-$Ca_2SiO_4$ as catalysts by TGA. For the three types of biomass tested,

Ni-CaO-$Ca_2SiO_4$ showed the catalytic effect, as reflected by a decrease in $E_\alpha$. However, for straw pyrolysis, Ni-$Ca_2SiO_4$ increased the activation energy, which might be due to the strong interaction of the catalyst with the metals in the ash of straw.

**Table 8.** Activation energies of different textile samples from Kissinger method.

| Sample | $E_\alpha$ (kJ/mol) |
|---|---|
| White polyester | 202.7 |
| White polyester (20% KOH) | 247.4 |
| White polyester (20% Zeolite) | 224.9 |
| White polyester (20% CaO) | 296.5 |
| White polyester (20% ZnO) | 345.5 |
| White cotton | 241.1 |
| White cotton (10%$K_2CO_3$) | 288.7 |
| White cotton (20%$K_2CO_3$) | 257.4 |
| White nylon | 218.9 |
| White nylon (20% ZnO) | 125.9 |

The $E_\alpha$ estimated using the KAS method is presented in Figures 10–12. The activation energy ($E_\alpha$) values of white polyester with ZnO across different fractional conversions ($\alpha$) were the highest among all tested catalysts. As illustrated in Figure 10, the values for the ZnO-catalyzed pyrolysis range from 400 kJ/mol to approximately 1000 kJ/mol at $\alpha$ = 0.8, which is significantly higher than the ranges observed for other catalysts (200–300 kJ/mol). Conversely, for the CaO catalyst at a fractional conversion of 0.9, the calculated activation energy drops to 0 kJ/mol. This near-zero value at the final stage of decomposition is attributed to a mathematical artifact in the isoconversional model fitting; at such high conversion levels, the remaining mass loss is negligible, leading to a loss of linear correlation in the Arrhenius plots. For white cotton with $K_2CO_3$, as shown in Figure 11, $E_\alpha$ had a broader range (100–300 kJ/mol). $E_\alpha$ for white nylon with ZnO was between 35 and 74 kJ/mol (Figure 12), which was much lower than the activation energy of undyed cotton and polyester using the KAS method.

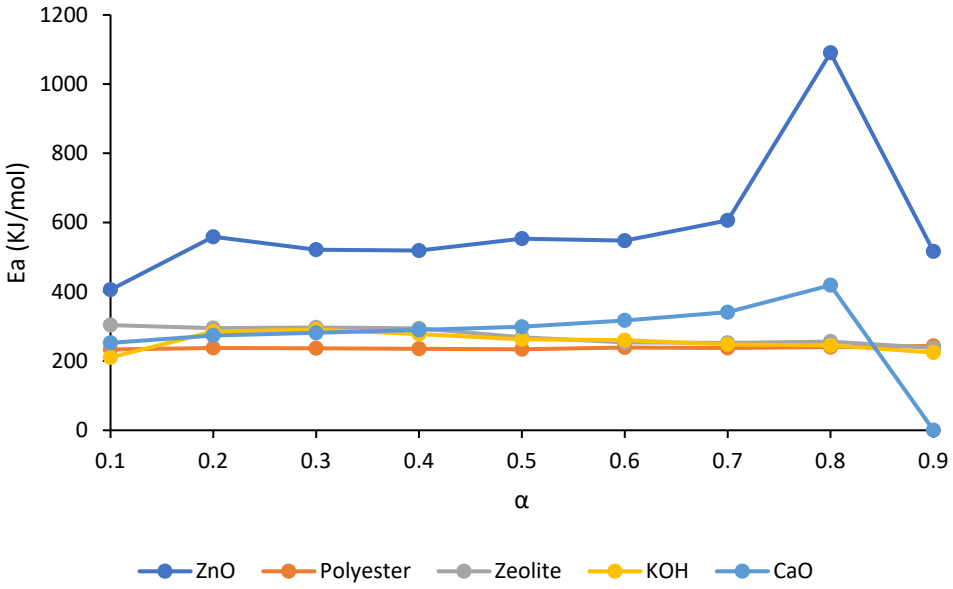


**Figure 10.** $E_\alpha$ of white polyester with catalysts at different fractional conversions from the KAS method.

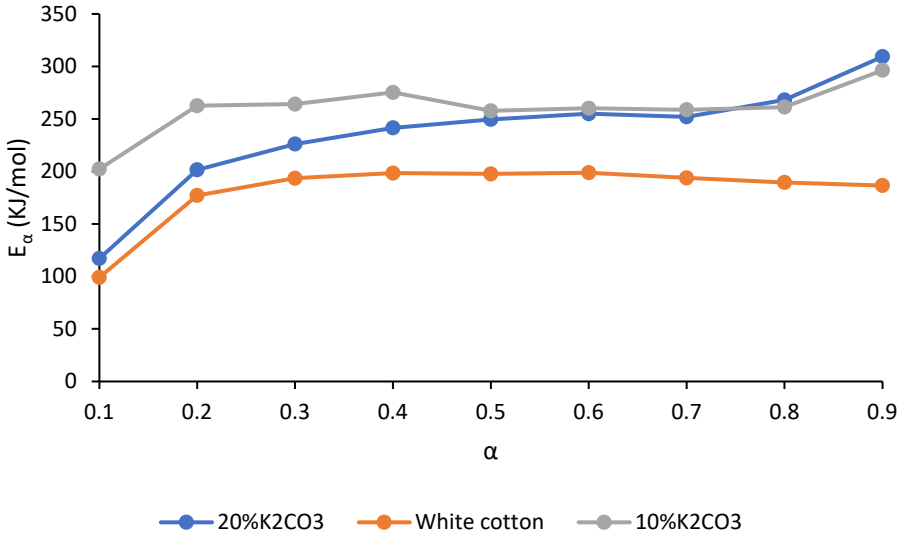


**Figure 11.** $E_\alpha$ of white cotton with catalysts at different fractional conversions from the KAS method.

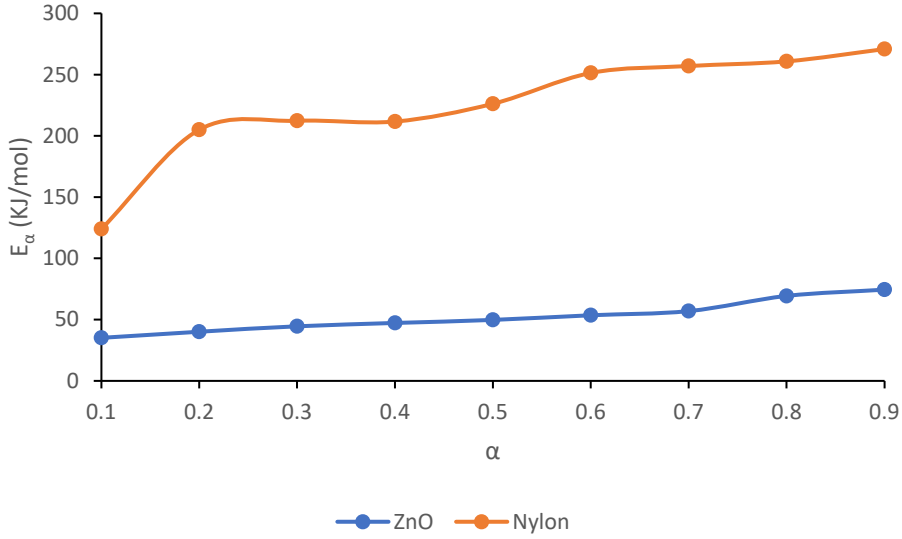


**Figure 12.** $E_\alpha$ of white nylon with 20% ZnO at different fractional conversions from the KAS method.

Chong et al. [34] aimed to assess kinetic parameters for the thermal decomposition of cellulose and palm empty fruit bunch fiber (EFBF) in the presence of calcium oxide (CaO), zinc oxide (ZnO) and magnesium oxide (MgO). Using these oxides, the average activation energy of EFBF decreased, where the most significant reduction was seen for the addition of 10 wt% of MgO (274.5 to 194.8 kJ/mol).

According to Table 5, using the FWO method, the activation energy of white cotton is lower than that of white polyester and white nylon (183 vs. 237 and 224 kJ/mol). Utilizing catalysts increased the activation energies of both polyester and cotton compared with the pyrolysis of pure samples (Table 9). However, white nylon with ZnO showed a 34% decrease in $E_\alpha$ compared to nylon alone. This suggests that ZnO is a very effective catalyst for the pyrolysis of nylon. A decrease in apparent activation energy suggests that the dominant decomposition pathway requires less energy, which is consistent with catalytic facilitation of key bond-breaking steps. For example, Lewis-acidic or redox-active metal oxides can weaken ester or amide linkages through coordination effects, while alkaline catalysts can promote base-catalyzed fragmentation and dehydration reactions. In addition, catalytic enhancement of volatile removal can reduce the extent of secondary reactions at the sample surface, effectively lowering the energy barrier inferred from TGA. Suami

et al. [35] used the FWO method to estimate the activation energy of the pyrolyzed polyester and cotton with and without $FeCl_2$. The $E_\alpha$ for cotton was 133 kJ/mol, while the value with the catalyst was 124 kJ/mol. Their result proved that the addition of $FeCl_2$ improved the pyrolysis rate of cotton and enhanced pyrolysis in the low-temperature range, whereas the activation energies of polyester with and without a catalyst were almost in the same range (203 and 205 kJ/mol, respectively).

**Table 9.** $E_\alpha$ (kJ/mol) of catalytic pyrolysis of white cotton, white nylon and white polyester at various fractional conversions ($\alpha$) by the FWO method.

| Sample | $\alpha$ | | | | | | | | | Average |
|---|---|---|---|---|---|---|---|---|---|---|
| | 0.1 | 0.2 | 0.3 | 0.4 | 0.5 | 0.6 | 0.7 | 0.8 | 0.9 | |
| Cotton with 10% $K_2CO_3$ | 202.0 | 259.6 | 261.3 | 272.0 | 255.4 | 257.8 | 256.5 | 259.1 | 292.8 | 257.4 |
| Cotton with 20% $K_2CO_3$ | 120.6 | 201.5 | 225.0 | 239.8 | 247.6 | 252.9 | 250.1 | 265.5 | 305.2 | 234.3 |
| Polyester with zeolite | 299.9 | 291.7 | 293.5 | 291.3 | 266.7 | 252.7 | 251.6 | 255.3 | 238.0 | 271.2 |
| Polyester with KOH | 210.7 | 282.2 | 287.9 | 275.5 | 260.9 | 258.7 | 247.1 | 244.6 | 225.4 | 254.8 |
| Polyester with ZnO | 400.4 | 540.3 | 472.1 | 491.3 | 468.2 | 482.5 | 546.1 | 763.2 | 479.1 | 515.9 |
| Polyester with CaO | 250.7 | 271.3 | 278.7 | 286.7 | 295.6 | 313.0 | 335.8 | 410.1 | N/A | 262.9 |
| Nylon with ZnO | 113.1 | 122.6 | 131.8 | 137.1 | 142.1 | 150.4 | 157.5 | 185.7 | 195.9 | 148.4 |

The heating rate may affect the balance of sample decomposition and the heat transfer process, because of the lag of sample temperature to the reactor temperature. No clear pattern is observed in Figures 13 and S1–S6 regarding the impact of heating rate on the extracted activation energy from different kinetic models, suggesting that there is little heat transfer limitation at the heating rates selected in this study. The mechanisms for the catalytic reaction of white polyester with KOH, zeolite and CaO followed the diffusion model (D1) ($E_\alpha$ = 250–270 kJ/mol). However, the proposed reaction models could not successfully describe the pyrolysis of white polyester with ZnO because of its high $E_\alpha$ (>500 kJ/mol). For catalytic pyrolysis of undyed cotton with 10 and 20% $K_2CO_3$, three-dimensional diffusion mechanisms of D3 and D4 appeared to match most. The mechanism model that closely matched the pyrolysis of white nylon with ZnO was R2 or R3. Chong et al. [34] discovered that CaO, MgO, and ZnO would not affect the mechanisms other than catalyzing the reactions. Mostly second-order chemical reaction and three-dimensional diffusion are the closest mechanisms to describe the decomposition of EFBF in the presence of oxide catalysts. The cellulose decomposition was controlled by a 1.5-order chemical reaction and a three-dimensional diffusion mechanism.

Kinetic compensation occurs when there is a strong and positive correlation between the pre-exponential factor A and activation energy $E_\alpha$ from the Arrhenius equation for a reaction between the same reactants under similar experimental settings or similar reactants under the same settings, even though those parameters should be independent. The kinetic compensatory effect has a few origins: (1) the chemical and physical characteristics of the reactants and the reaction process; (2) the measurement settings in the thermal analysis experiment; (3) the calculation and approaches of experimental data processing [36].

According to Figures 14 and S7–S9, there exist strong positive compensation effects among activation energies and pre-exponential factors in the pyrolysis of textiles with and without catalysts. Those results prove that changes in activation energy were compensated for partially by changes in the pre-exponential factor. Similar results were achieved in the study of compensation effects of pyrolyzed ramie during various thermal treatments; the linear relationship $\lg A = -1.3515 + 0.0808\ E_\alpha$ ($R^2$ = 0.9999) for ramie was determined [12]. The decrease in $E_\alpha$ indicates a lesser degree of dependence or sensitivity of the pyrolysis reaction rate on the temperature, but not necessarily a higher reaction rate, and vice versa.

It is clearly observed in this study that the reaction rate constants increase significantly with the introduction of catalysts, as shown in Table 10 and Figures S10–S12 (except for white nylon). The increase in reaction rate can be attributed to both the improvement of heat transfer for those poorly thermally conductive textile samples and the intrinsic catalytic effect on the cracking of organic vapors, which accelerates the removal of decomposed products from the sample surface.

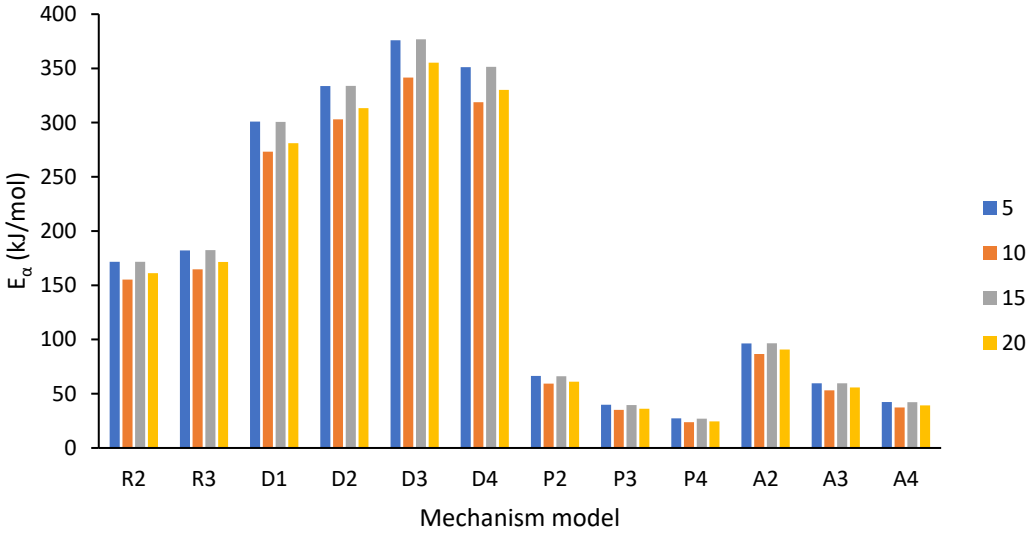


**Figure 13.** Relationship among heating rate, activation energy and reaction mechanisms for pyrolysis of white polyester with KOH.

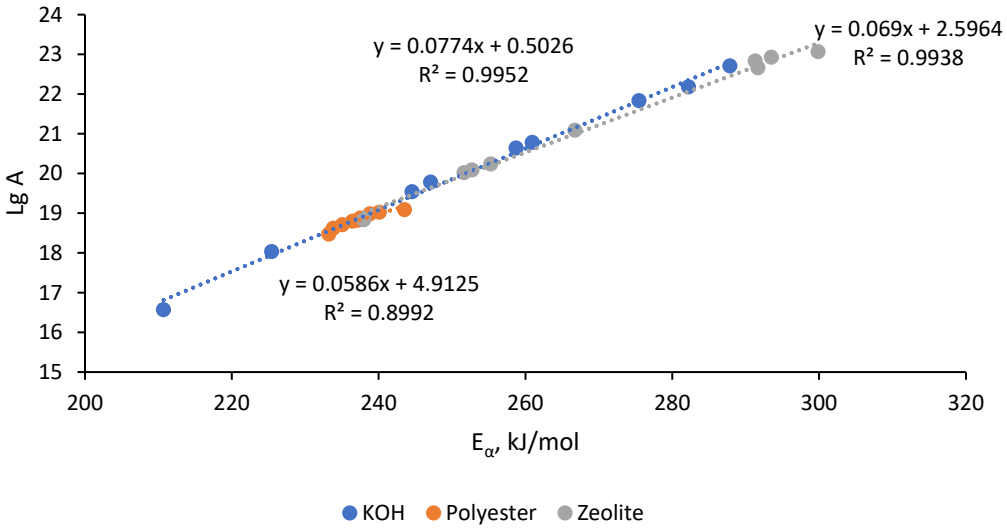


**Figure 14.** Compensation effect between pre-exponential factor and activation energy of pyrolyzed white polyester with KOH and zeolite.

In several cases, catalyst addition increased the apparent activation energy. This does not necessarily contradict the catalytic promotion of pyrolysis. Under non-isothermal TGA conditions, the calculated activation energy is an "apparent" value reflecting the dominant overall pathway rather than a single elementary step. A higher apparent $E_\alpha$ may indicate that the catalyst shifts the mechanism toward a pathway that is more temperature-sensitive (e.g., enhanced char-forming reactions, stronger catalyst–intermediate interactions, or diffusion-influenced decomposition). Moreover, the kinetic compensation effect observed in this work indicates that increases in $E_\alpha$ can be accompanied by substantial increases in the pre-exponential factor (A) or turnover frequency, resulting in higher overall reaction

rate constants despite higher $E_\alpha$. Therefore, evaluation of both $E_\alpha$ and A (or reaction rate constant k) is necessary to assess catalytic effectiveness.

**Table 10.** Reaction rate constant, (k) of white polyester with and without catalyst.

| Temperature (°C) | k | | | | |
|---|---|---|---|---|---|
| | **Polyester** | **Zeolite** | **KOH** | **CaO** | **ZnO** |
| 100 | $1.25 \times 10^{11}$ | $4.36 \times 10^{12}$ | $2.53 \times 10^{14}$ | $1.75 \times 10^{18}$ | $6.53 \times 10^{21}$ |
| 200 | $1.26 \times 10^{11}$ | $4.42 \times 10^{12}$ | $2.57 \times 10^{14}$ | $1.78 \times 10^{18}$ | $6.68 \times 10^{21}$ |
| 300 | $1.27 \times 10^{11}$ | $4.47 \times 10^{12}$ | $2.60 \times 10^{14}$ | $1.81 \times 10^{18}$ | $6.79 \times 10^{21}$ |
| 400 | $1.28 \times 10^{11}$ | $4.50 \times 10^{12}$ | $2.62 \times 10^{14}$ | $1.82 \times 10^{18}$ | $6.86 \times 10^{21}$ |
| 500 | $1.29 \times 10^{11}$ | $4.52 \times 10^{12}$ | $2.63 \times 10^{14}$ | $1.84 \times 10^{18}$ | $6.92 \times 10^{21}$ |
| 600 | $1.29 \times 10^{11}$ | $4.54 \times 10^{12}$ | $2.64 \times 10^{14}$ | $1.85 \times 10^{18}$ | $6.96 \times 10^{21}$ |
| 700 | $1.30 \times 10^{11}$ | $4.55 \times 10^{12}$ | $2.65 \times 10^{14}$ | $1.85 \times 10^{18}$ | $6.99 \times 10^{21}$ |

## 4. Conclusions

Pyrolysis of cotton, polyester and nylon was carried out in a TGA. Catalysts increased the pre-exponential factor significantly, leading to an increased reaction rate and rate constant. Except for white nylon, catalysts increased the activation energies of pyrolysis reactions of undyed polyester and cotton, making the reactions more sensitive to temperature. There exists a strong compensation effect in the catalytic pyrolysis of white polyester, white nylon and white cotton. Overall, cotton, polyester, and nylon each show good suitability for catalytic pyrolysis, though with different strengths. Cotton decomposes at the lowest temperatures, making it relatively easy to break down, but its higher activation energy means it benefits strongly from catalysts like $K_2CO_3$ to enhance efficiency. Polyester is the most favorable overall, with the lowest activation energies and stable decomposition behavior, though catalyst choice is critical since ZnO can hinder rather than help. Nylon requires higher temperatures but becomes highly suitable when paired with ZnO, which dramatically reduces its activation energy and boosts reactivity. Taken together, the three fibers have overlapping decomposition ranges, making them thermally compatible for co-processing, with careful catalyst selection ensuring effective conversion and synergy. Although this work is based on TGA measurements, the obtained kinetic trends provide valuable guidance for selecting catalysts and operating temperature ranges for future bench- and pilot-scale pyrolysis studies involving real textile waste streams. The use of robust catalysts (e.g., CaO or ZnO) offers a path toward high-quality bio-oil production in fluidized bed reactors. Future work should focus on the mechanical separation of catalysts for regeneration and the performance of these systems under continuous feed conditions with heterogeneous post-consumer waste. Further study integrating product analysis and surface characterization of spent catalysts will help to elucidate detailed reaction pathways.

**Supplementary Materials:** The following supporting information can be downloaded at: https://www.mdpi.com/article/10.3390/chemengineering10050065/s1.

**Author Contributions:** Writing—original draft, P.A. and T.W.; Writing—review and editing, P.A., T.W. and X.B.; Formal analysis, P.A.; Conceptualization, P.A. and X.B.; Resources, M.S., P.S. and X.B.; Methodology, M.S., P.S. and X.B.; Investigation, S.C.; Data curation, S.C.; Supervision, X.B. All authors have read and agreed to the published version of the manuscript.

**Funding:** The authors are grateful to a grant from Mathematics of Information Technology and Complex Systems (Mitacs) and Lululemon Inc. to support the exploration of thermochemical recycling of textile wastes.

**Data Availability Statement:** The data presented in this study are available in Supplementary Materials. Data can also be requested from X.B. or P.A.

**Conflicts of Interest:** T.W. and P.S. were employed by Lululemon. The remaining authors declare that the research was conducted in the absence of any commercial or financial relationships that could be construed as a potential conflict of interest.

## References


1. Pure Waste Organization. Available online: https://www.purewaste.com/ (accessed on 5 May 2026).
2. Liang, X.; Ning, X.A.; Chen, G.; Lin, M.; Liu, J.; Wang, Y. Concentrations and speciation of heavy metals in sludge from nine textile dyeing plants. *Ecotoxicol. Environ. Saf.* **2013**, *98*, 128–134. [CrossRef]
3. Henry, B.; Laitala, K.; Klepp, I.G. Microfibres from apparel and home textiles: Prospects for including microplastics in environmental sustainability assessment. *Sci. Total Environ.* **2019**, *652*, 483–494. [CrossRef]
4. Singh, R.P.; Mishra, S.; Das, A.P. Synthetic microfibers: Pollution toxicity and remediation. *Chemosphere* **2020**, *257*, 127199. [CrossRef]
5. Yousef, S.; Eimontas, J.; Striūgas, N.; Tatariants, M.; Abdelnaby, M.A.; Tuckute, S.; Kliucininkas, L. A sustainable bioenergy conversion strategy for textile waste with self-catalysts using mini-pyrolysis plant. *Energy Convers. Manag.* **2019**, *196*, 688–704. [CrossRef]
6. Nunes, L.; Matias, J.; Catalão, J. Biomass in the generation of electricity in Portugal: A review. *Renew. Sustain. Energy Rev.* **2017**, *71*, 373–378. [CrossRef]
7. Perkins, G.; Bhaskar, T.; Konarova, M. Process development status of fast pyrolysis technologies for the manufacture of renewable transport fuels from biomass. *Renew. Sustain. Energy Rev.* **2018**, *90*, 292–315. [CrossRef]
8. Lee, H.S.; Jung, S.; Lin, K.-Y.A.; Kwon, E.E.; Lee, J. Upcycling textile waste using pyrolysis process. *Sci. Total Environ.* **2023**, *859*, 160393. [CrossRef]
9. Arjona, L.; Barrós, I.; Montero, Á.; Solís, R.R.; Pérez, A.; Martín-Lara, M.Á.; Blázquez, G.; Calero, M. Pyrolysis of textile waste: A sustainable approach to waste management and resource recovery. *J. Environ. Chem. Eng.* **2024**, *12*, 114730. [CrossRef]
10. Chen, Q.; Zhao, X.; Wang, N.; Wu, H.; Xu, Q. Fast pyrolysis of waste textiles: Product distribution, formation of hazardous by-products, and resource recovery pathways. *Waste Manag.* **2026**, *211*, 115293. [CrossRef] [PubMed]
11. Moltó, J.; Font, R.; Conesa, J.A.; Martín-Gullón, I. Thermogravimetric analysis during the decomposition of cotton fabrics in an inert and air environment. *J. Anal. Appl. Pyrolysis* **2006**, *76*, 124–131. [CrossRef]
12. Zhu, F.; Feng, Q.; Xu, Y.; Liu, R.; Li, K. Kinetics of pyrolysis of ramie fabric wastes from thermogravimetric data. *J. Therm. Anal. Calorim.* **2015**, *119*, 651–657. [CrossRef]
13. Wen, C.; Wu, Y.; Chen, X.; Jiang, G.; Liu, D. The pyrolysis and gasification performances of waste textile under carbon dioxide atmosphere. *J. Therm. Anal. Calorim.* **2017**, *128*, 581–591. [CrossRef]
14. Wu, Y.; Wen, C.; Chen, X.; Jiang, G.; Liu, G.; Liu, D. Catalytic pyrolysis and gasification of waste textile under carbon dioxide atmosphere with composite Zn-Fe catalyst. *Fuel Process. Technol.* **2017**, *166*, 115–123. [CrossRef]
15. Artetxe, M.; Lopez, G.; Amutio, M.; Elordi, G.; Olazar, M.; Bilbao, J. Operating conditions for the pyrolysis of poly-(ethylene terephthalate) in a conical spouted-bed reactor. *Ind. Eng. Chem. Res.* **2010**, *49*, 2064–2069. [CrossRef]
16. Xie, M.; Cheng, M.; Yang, Y.; Huang, Z.; Zhou, T.; Zhao, Y.; Xiao, P.; Cen, Q.; Liu, Z.; Li, B. A review on catalytic pyrolysis of textile waste to high-value products: Catalytic mechanisms, products application and perspectives. *Chem. Eng. J.* **2024**, *498*, 155120. [CrossRef]
17. Kissinger, H.E. Variation of peak temperature with heating rate in differential thermal analysis. *J. Res. Natl. Bur. Stand.* **1956**, *57*, 217–221. [CrossRef]
18. Akahira, T.; Sunuse, T. Joint convention of four electrical institutes. *Res. Rep. Chiba Inst. Technol.* **1971**, *16*, 22–31.
19. Flynn, J.H.; Wall, L.A. A quick, direct method for the determination of activation energy from thermogravimetric data. *J. Polym. Sci. Part B Polym. Lett.* **1966**, *4*, 323–328. [CrossRef]
20. Ozawa, T. A new method of analyzing thermogravimetric data. *Bull. Chem. Soc. Jpn.* **1965**, *38*, 1881–1886. [CrossRef]
21. Coats, A.W.; Redfern, J. Kinetic parameters from thermogravimetric data. *Nature* **1964**, *201*, 68–69. [CrossRef]
22. Vyazovkin, S.; Wight, C.A. Kinetics in solids. *Annu. Rev. Phys. Chem.* **1997**, *48*, 125–149. [CrossRef] [PubMed]
23. Athanasopoulos, P.; Zabaniotou, A. Post-consumer textile thermochemical recycling to fuels and biocarbon: A critical review. *Sci. Total Environ.* **2022**, *834*, 155387. [CrossRef] [PubMed]
24. Al-Salem, S.; Khan, A. On the degradation kinetics of poly (ethylene terephthalate)(PET)/poly (methyl methacrylate)(PMMA) blends in dynamic thermogravimetry. *Polym. Degrad. Stab.* **2014**, *104*, 28–32. [CrossRef]
25. Sakata, Y.; Uddin, M.A.; Koizumi, K.; Murata, K. Thermal degradation of polyethylene mixed with poly (vinyl chloride) and poly (ethyleneterephthalate). *Polym. Degrad. Stab.* **1996**, *53*, 111–117. [CrossRef]

26. Çepelioğullar, Ö.; Pütün, A.E. Thermal and kinetic behaviors of biomass and plastic wastes in co-pyrolysis. *Energy Convers. Manag.* **2013**, *75*, 263–270. [CrossRef]
27. Ko, K.-H.; Rawal, A.; Sahajwalla, V. Analysis of thermal degradation kinetics and carbon structure changes of co-pyrolysis between macadamia nut shell and PET using thermogravimetric analysis and 13C solid state nuclear magnetic resonance. *Energy Convers. Manag.* **2014**, *86*, 154–164. [CrossRef]
28. Girija, B.; Sailaja, R.; Madras, G. Thermal degradation and mechanical properties of PET blends. *Polym. Degrad. Stab.* **2005**, *90*, 147–153. [CrossRef]
29. Alhulaybi, Z.; Dubdub, I. Comprehensive kinetic study of PET pyrolysis using TGA. *Polymers* **2023**, *15*, 3010. [CrossRef]
30. Matsumura, M.; Inagaki, J.; Yamada, R.; Tashiro, N.; Ito, K.; Sasaki, M. Material Separation from Polyester/Cotton Blended Fabrics Using Hydrothermal Treatment. *ACS Omega* **2024**, *9*, 13125–13133. [CrossRef]
31. Yousef, S.; Eimontas, J.; Striūgas, N.; Praspaliauskas, M.; Abdelnaby, M.A. Pyrolysis behavior of non-textile components (buttons) and their kinetic analysis using artificial neural network. *J. Anal. Appl. Pyrolysis* **2025**, *186*, 106880. [CrossRef]
32. Osman, A.I.; Farrell, C.; Al-Muhtaseb, A.H.; Al-Fatesh, A.S.; Harrison, J.; Rooney, D.W. Pyrolysis kinetic modelling of abundant plastic waste (PET) and in-situ emission monitoring. *Environ. Sci. Eur.* **2020**, *32*, 112. [CrossRef]
33. Yang, H.; Ji, G.; Clough, P.T.; Xu, X.; Zhao, M. Kinetics of catalytic biomass pyrolysis using Ni-based functional materials. *Fuel Process. Technol.* **2019**, *195*, 106145. [CrossRef]
34. Chong, Y.Y.; Ng, H.K.; Lee, L.Y.; Gan, S.; Thangalazhy-Gopakumar, S. Kinetics and mechanisms for catalytic pyrolysis of empty fruit bunch fibre and cellulose with oxides. *SN Appl. Sci.* **2020**, *2*, 1464. [CrossRef]
35. Suami, A.; Minami, K.; Kobayashi, N.; Itaya, Y. The effect of catalyst on pyrolysis behavior of cotton and PEs for waste clothes reusing. *Mech. Eng. J.* **2024**, *11*, 23-00489. [CrossRef]
36. Koga, N. A review of the mutual dependence of Arrhenius parameters evaluated by the thermoanalytical study of solid-state reactions: The kinetic compensation effect. *Thermochim. Acta* **1994**, *244*, 1–20. [CrossRef]